# Self-bending of the coupled spatial soliton pairs in a photorefractive medium with drift and diffusion nonlinearity

Victor Aleshkevich and Yaroslav Kartashov*
*Chair of General Physics, Physics Department, M. V. Lomonosov Moscow State University, Vorobiovy gory, 119899 Moscow, Russia*

Victor Vysloukh
*Centre de Investigaciones en Ingeniesia y Ciencias Aplicadas, Universidad Autonoma del Estado de Morelos Dirección, CP 62210 Cuernavaca, Morelos, Mexico*

(Received 28 February 2000; revised manuscript received 25 September 2000; published 19 December 2000)

The propagation of two incoherently coupled laser beams (coupled soliton pairs) in the photorefractive crystal with drift and diffusion components of nonlinear response is investigated. By the effective particles method we have shown that not only the well-known Manakov's soliton pairs but also asymmetric pairs can propagate undistorted in photorefractive crystal with diffusion nonlinearity along the parabolic trajectory for the definite relations of propagation constants. We numerically found the exact profiles of the specific multihump soliton solutions that are possible only in the photorefractive medium with nonlocal diffusion response. The stability properties and specific features of pair collisions are analyzed.

DOI: 10.1103/PhysRevE.63.016603 PACS number(s): 42.65.Wi, 42.65.Jx, 42.65.Tg

## I. INTRODUCTION

Spatial solitons in photorefractive crystals (PRC) have been of growing interest during the past several years. At least three generic types of the planar ($(1+1)$-dimensional) photorefractive solitons have been predicted and observed to the date. First, the quasi-steady-state solitons exist in PRC when an external applied field is slowly being screened [1,2]. The second type is the so-called screening solitons that occur in a steady state when the external field is nonuniformly screened [3–8]. The third type is the photovoltaic solitons [9]. Photorefractive spatial solitons can occur at microwatt power levels. Therefore PRC's are extremely suitable materials for nonlinear switching optical devices construction. The concept of such devices is based on the fact that the soliton is a fundamental mode of the optical waveguide which it creates in a photorefractive medium. Structures formed by intersecting waveguides (i.e., by colliding coherent [10–13] and incoherent [14,15] solitons) are especially attractive from the practical point of view.

Another intriguing issue—the cross-modulation coupling of incoherent solitonlike $(1+1)$ dimensional beams in photorefractive media exhibiting purely drift (quasilocal) nonlinearity of the Kerr type—also was subjected to the careful consideration (see [4] and references cited herein). The Kerr-type regime of nonlinearity can be realized in photorefractive crystal under the influence of the high static external electric field for a relatively wide (20–50 $\mu$m) laser beams if photoinduced conductivity is considerably less than the dark conductivity (i.e., when the intensity of the laser beam $I$ is small compared with the dark irradiance level $I_{\mathrm{dark}}$). In this case the saturable response of the photorefractive medium can be described by the first term of the expansion on small parameter $I/I_{\mathrm{dark}}$, i.e., by Kerr-type law. It should be noted that the effective level of the dark conductivity could be considerably increased due to the introduction of the external background illumination. Mathematical justification of the applicability of the Kerr-type model for the photorefractive medium can be found in [5] (see for example Eq. (24)) and [16] (Eq. (17)). The further decrease of the transverse beam extent causes the increase of the influence of the nonlocal diffusion component of PRC response leading to the self-bending effect [17–21]. The influence of this nonlocal component on the single laser beams shaping and interaction was examined in great detail for the case of the self-bending of the one-component photorefractive solitons [22], as well as for the case of temporal solitons in the medium with Raman component of the nonlinear response [23]. The behavior of the two incoherently coupled beams in PRC with nonlocal response calls however for the separate consideration. In the present paper we concentrate on the self-bending of two-component optical solitons produced by the incoherent cross-modulation coupling of $(1+1)$ dimensional laser beams with the specific shapes. The interest to this problem is motivated not only by the reason of theoretical generalization of the previous results but also by possible applications in devices of light-by-light control and for pure optical waveguiding. Multicomponent solitons offer new possibilities in the flexible changing relation between the maximal increment of the refractive index and the nonlinear waveguide width [4].

Below the results of theoretical analysis and computer simulation of the influence of nonlocal component of nonlinear response on the coupled soliton pair propagation and interaction are presented. Using the effective particle method we look for the trajectories of the coupling beams having the input profiles given by the well-known solutions for the case of Kerr-type nonlinearity. Further the exact profiles for the self-bending two-component spatial solitons are presented. Stability of these solutions and specific features of their collisions are also examined by computer simulation.

*Corresponding author. FAX: (095) 939-14-89. Email: azesh@gateway.phys.msu.su

 

## II. THEORETICAL MODEL

To describe the propagation of the coupled soliton pair in the photorefractive medium with drift and diffusion nonlinearity we apply the well established technique which uses the standard shortened wave equation completed with a set of charge-transport equations describing the photorefractive effect in a nonlinear medium [3–8]. Further we consider the case when two laser beams sharing the same polarization and having practically the same wavelengths launched onto the input face of the photorefractive crystal with rather large characteristic response time $\tau_{\rm rel}$ so, that the wave numbers difference $\Delta k$ greatly exceeds $1/c\tau_{\rm rel}$. Thus, no stationary interference pattern can form within a time scale comparable with the response time of the crystal and nonlinear refractive index perturbation is defined only by the modal sum of intensities of the laser beams. Under this assumption the joint solution of the shortened wave equation and charge-transport equations for the photorefractive crystals with rather large dark conductivity and a weak diffusion current results in the following system of the coupled wave equations for the normalized complex field amplitudes $q_{1,2}(\eta,\xi)$:

$$i\frac{\partial q_{1,2}}{\partial \xi}=-\frac{1}{2}\frac{\partial^2 q_{1,2}}{\partial \eta^2}-q_{1,2}(|q_1|^2+|q_2|^2)+\mu q_{1,2}\frac{\partial}{\partial \eta}(|q_1|^2+|q_2|^2). \tag{1}$$

Here $\eta=x/x_0$ is the normalized transverse coordinate; $x_0$ is an arbitrary spatial scale; $\xi=z/L_d$ is the normalized propagation distance; $L_d=kx_0^2$ is the diffraction length, corresponding to $x_0$; $k=n_0\omega/c$ is the wave number; $n_0$ is the unperturbed refraction index; $\omega$ is the central radiation frequency; $q_{1,2}(\eta,\xi)=A_{1,2}(\eta,\xi)(R_{dr}/I_d)^{1/2}$; $A_{1,2}(\eta,\xi)$ is the amplitude of the light field; $R_{dr}=L_d/L_r$; $L_r=2/(kr_{\rm ef}{n_0}^2E_0)$ is the nonlinear refraction length; $r_{\rm ef}$ is the effective electro-optic coefficient; $E_0$ is the static electric field applied to PRC in the transverse $x$-direction; $I_d$ describes the dark conductivity of the PRC; parameter $\mu$ describes the magnitude of the nonlocal diffusion component of PRC response. The sign of $\mu$ depends on the direction of the externally applied electric field $E_0$. The last term in the right side of Eq. (1) describes the self-bending effects resulting due to the energy transfer from the low- to the high-frequency spatial components. The first term in the right part of Eq. (1) describes the diffraction spreading of the beams, the second one describes its self-focusing due to the drift component of nonlinear response which is quasilocal in the one-dimensional case.

Equation (1) is analogous to that describing the Raman self-frequency shift in the time domain [24,25]. In the latter case coordinate $\eta$ corresponds to the normalized running time $(t\text{-}z/c)/\tau_0$; $\xi$ corresponds to the longitudinal coordinate $z/L_d$ normalized by the dispersion length $L_d=\tau_0^2/|k''|$; parameter $\mu$ is proportional to the ratio $\tau_R/\tau_0$, where $\tau_R$ is the Raman response characteristic time. Thus the model considered here could be also referred to the case of temporal solitons in Kerr medium in the presence of Raman amplification [23].

We search for the solution of the system (1) in the standard way introducing the real envelopes $\rho_{1,2}$ so that $q_{1,2}(\eta,\xi)=\rho_{1,2}(\eta)\exp(ib_{1,2}\xi)$. After the substitution one can obtain the following system of the coupled nonlinear differential equations of the second order:

$$\frac{d^2\rho_{1,2}}{d\eta^2}=2\rho_{1,2}\left(b_{1,2}-(\rho_1{}^2+\rho_2{}^2)+\mu\frac{d}{d\eta}(\rho_1{}^2+\rho_2{}^2)\right). \tag{2}$$

The latter system can be integrated for example with the aid of methods of the inverse scattering transform (IST) only for the case of the purely drift nonlinearity, i.e., when parameter $\mu=0$. There are two well-known types of bright-soliton solutions (besides the trivial case when one of the components is zero) of the system (2) with zero $\mu$ had been presented to the date. The first one (the one-soliton solution of the Manakov model) is possible for the equal values of the propagation constants $b_1=b_2=b$ and can be written in the following way [26]:

$$\rho_1=(2b)^{1/2}\cos\varphi\,\mathrm{sech}[(2b)^{1/2}\eta],\qquad \rho_2=(2b)^{1/2}\sin\varphi\,\mathrm{sech}[(2b)^{1/2}\eta], \tag{3}$$

where $\varphi$ is arbitrary projection angle. The constituents of the solution (3) are purely symmetric and have the same functional dependence on $\eta$. In our case of coupled soliton pairs these two components can be considered as the $\varphi$ projections of the fundamental bright-soliton envelope. Such stable pairs, which have been first realized as a stable pair of laser pulses with orthogonal polarization in nonlinear waveguides [27], have been observed recently in PRC [28]. The second type of bright-soliton solution (the two-soliton solution of the Manakov model) is possible for the different values of propagation constants and for example for the case of $b_1>b_2$ have the following form [29,30]:

$$\rho_1=\frac{[2(b_1-b_2)]^{1/2}\cosh[d_2(\eta-\eta_s)]}{\cosh[d_1\eta]\cosh[d_2(\eta-\eta_s)]-(b_2/b_1)^{1/2}\sinh[d_1\eta]\sinh[d_2(\eta-\eta_s)]},$$

$$\rho_2=\frac{[2(b_1-b_2)]^{1/2}\sinh[d_1\eta]}{(b_1/b_2)^{1/2}\cosh[d_1\eta]\cosh[d_2(\eta-\eta_s)]-\sinh[d_1\eta]\sinh[d_2(\eta-\eta_s)]}. \tag{4}$$

Here parameter $\eta_s$ describes the shift between centers of constituents of the pair and we introduced the notations $d_1=(2b_1)^{1/2}$ and $d_2=(2b_2)^{1/2}$. In terms of popular approach it can be shown that the first component of (4) is a zero-order linear mode of the self-induced waveguide and the second component is the first-order linear mode. One can see that in contradistinction with (3) there exist three parameters describing the soliton profile. In general the solution of the $N$ coupled nonlinear Shrödinger equations is defined by $2N$-1 free parameters: $N$ propagation constants describing the amplitudes of the solitons and $N$-1 beam center coordinates describing the beam center positions, i.e., coupling between constituents. Thus with increase of parameter $\eta_s$ the asymmetry of the solution (4) increases finally resulting in decoupling of the pair into the two independent solitons when $\eta_s \rightarrow \infty$. Both solutions (3) and (4) can be obtained in terms of IST and are known to be structurally stable with respect to the small and collision-type perturbations [30,31]. Nevertheless, one should take into account that in any real experiment the needed 1D diffraction and self-interaction can be realized only by using slit beams with uniform field distribution in direction orthogonal to $\xi$ and $\eta$. In doing so, one must take into account a possibility of beam filamentation, which can develop on PRC length due to modulation instability [32,33].

The inclusion of the diffusion term in the right side of Eq. (2) (the case of nonzero $\mu$) drastically changes the picture even for the very small value of $\mu$. No more nondistorting in propagation process localized soliton solutions are possible. For the case of equal propagation constants the specific nondiffracting solution can be expressed in terms of two coupled bright shock waves which can be thought as a $\varphi$ projections of the fundamental shock wave [16] analogously to the one-component Manakov solitons. For the nonequal propagation constants the solution has an even more complicated form of the coupled bright and dark shock waves. But further we are interested only in the localized self-bend soliton pairs that can be found with the aid of two methods presented below (effective particles method and transformation into the parabolic coordinate system) completed one another.

### III. THE EFFECTIVE PARTICLES METHOD

In this section we consider the trajectories of the pairing beams having the input profiles presented by (3) and (4) and launched into the PRC with a nonlocal component of nonlinear response. The propagation trajectory can be easily found with the aid of the method of the effective particles which is frequently used in quantum mechanics and enables one to obtain the trajectories of particle motion in different potentials if the evolution of the localized particle wave function is governed by the equation of the type (1) (perturbed nonlinear Shrödinger equation). With this method one can obtain that the localized (that means both $q_{1,2}(\eta \rightarrow \pm\infty, \xi)=0$ and $\partial q_{1,2}(\eta \rightarrow \pm\infty, \xi)/\partial\eta=0$) pairing beams trajectories in the PRC with nonlocal component in nonlinear response is given by

$$w_{1,2}\frac{d^2\eta_{1,2}}{d\xi^2}=\mu\int_{-\infty}^{\infty}\frac{d}{d\eta}\rho_{1,2}^2\frac{d}{d\eta}(\rho_1{}^2+\rho_2{}^2)d\eta. \qquad (5)$$

Here we introduced the beam powers $w_{1,2}=\int_{-\infty}^{\infty}\rho_{1,2}{}^2 d\eta$ and beam center coordinates

$$\eta_{1,2}=\int_{-\infty}^{\infty}\rho_{1,2}{}^2\eta d\eta \Big/ \int_{-\infty}^{\infty}\rho_{1,2}{}^2 d\eta. \qquad (6)$$

As discussed earlier, $\rho_{1,2}$ is the real beam shapes (for example unperturbed profiles given by (3) and (4)). One can see from Eq. (5) that the constituents of the pair move along the parabolic trajectories

$$\eta_{1,2}=a_{1,2}\xi^2/2, \qquad (7)$$

which is defined by both the intensity of each constituent and common intensity profile. If the pair constituents start their propagation along the different trajectories then the pair decouples and expression (5) is valid only at the initial stage of propagation, due to the strong perturbation of the beam profiles through the decoupling. But the opposite case of stable propagation enables one to readily obtain the approximate (it is expected that for the typical experimental values of $\mu \sim 0.1$ the relative shape transformation in the propagation process is of the order of $\mu$) analytical profiles of the pair constituents.

First we considered the one-soliton solution (3) and obtained that as for the case of the single beam [22–25] the Manakov pair shows the stable propagation along the parabolic trajectory with $a_{1,2}=(32/15)\mu b^2$ despite the amplitude difference of the pair constituents. This is due to the fact that the given constituent ''feels'' the common intensity profile (which is the same for the different projection angles $\varphi$) but not only intensity of the other component. The exact profiles of the one-soliton solutions that become slightly asymmetric due to the diffusion component of nonlinear response will be presented in the next section. Besides it will be shown that the presence of even weak diffusion component results in the appearance of the specific multihump one-soliton solutions allowing different projection states just as Manakov solitons.

The rather complicated expressions of the beam shapes for the second asymmetric solution (4) does not enable one to obtain an analytical expression for the parabolic coefficients and the only way is a numerical integration. Figure 1 shows the dependence of the parabolic coefficients difference $a_1$-$a_2$ on the values of propagation constants $b_1$ and $b_2$ for the zero shift $\eta_s$. The plateau is due to the chosen above relation $b_1>b_2$. One can see that for the definite values of propagation constants $b_{1,2}$ it is possible the regime of the stable pair propagation, i.e., condition $a_1$-$a_2=0$ is satisfied. With increase of the beam centers shift $\eta_s$ the region of values of $b_{1,2}$ in which the stable pair propagation occurs significantly suppresses. The values of $b_1$ and $b_2$ corresponding to the stable pair propagation (the geometrical place of points corresponding to the condition $a_1$-$a_2=0$) for the different shifts $\eta_s$ presented in Fig. 2. One can see that all possible $b_{1,2}$ situated within the angle formed by two straight lines: $b_2=b_1$ (the existence condition for the asymmetric soliton state) and $b_2=0.414b_1$ (specific boundary condition for the two-soliton solution of the Manakov model). Using the values of $b_1$, $b_2$, and $\eta_s$ defined from Fig.

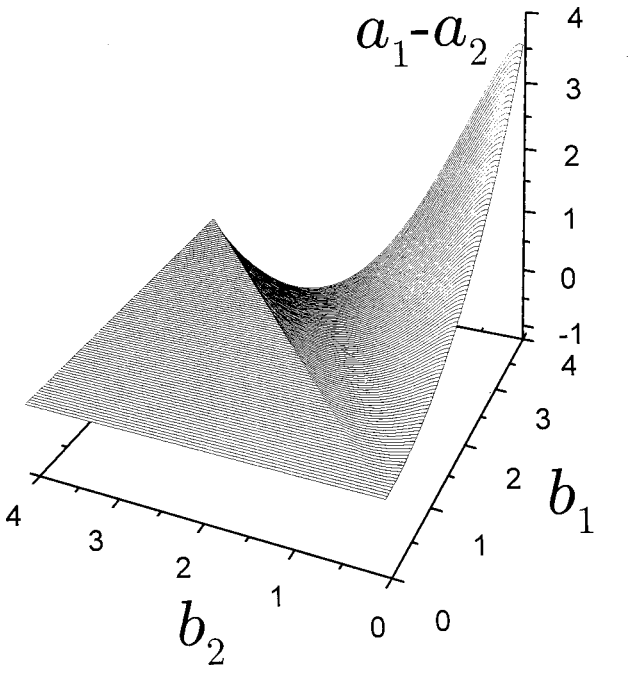


FIG. 1. Dependence of the parabolic coefficients difference $a_1$-$a_2$ for the constituents of two-soliton solution on the values of propagation constants $b_1$ and $b_2$ for the zero soliton centers shift $\eta_s$. All quantities are plotted in arbitrary dimensionless units.

2 one can readily obtain from (4) the approximate analytical expressions for the stable self-bend pairs profile. The latter method works especially well for the case of moderate propagation constants difference $b_1$-$b_2$<0.8 because for the higher values of $b_1$-$b_2$ (i.e., with increase of soliton energy) the additional energy insight due to the presence of diffusion nonlinearity becomes more pronounced and can result in the pair decoupling after the propagation over the big (~10 diffraction lengths) distance in PRC. Besides the calculation of

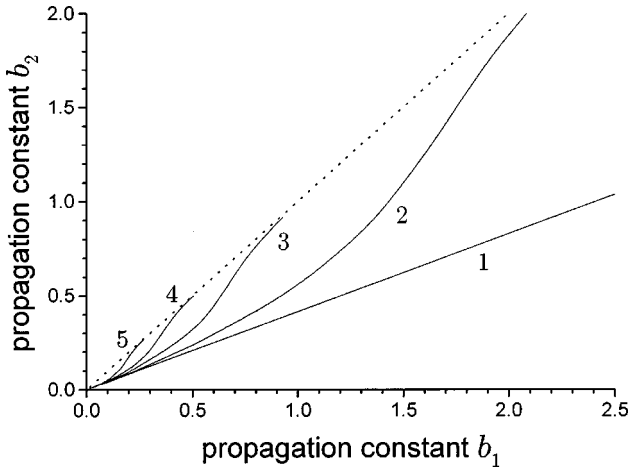


FIG. 2. The relation between propagation constants $b_1$ and $b_2$ corresponding to the stable two-soliton pair propagation (condition $a_1$-$a_2$=0) for the soliton centers shift $\eta_s$=0 (1); 0.5 (2); 0.8 (3); 1.1 (4); 1.5 (5). The existence condition for the asymmetric two-soliton state ($b_1$>$b_2$) is depicted by dotted line. All quantities are plotted in arbitrary dimensionless units.

the trajectory calls for the additional numerical integration. The next supplementing method enables one to overcome difficulties with trajectory calculation.

## IV. THE EXACT PAIR SHAPES

For an arbitrary (the really achievable experimental values are up to 0.4) value of parameter $\mu$ describing the strength of the diffusion component of PRC response we look for the stable self-bend soliton pair profile in the following form:

$$q_{1,2}(\eta,\xi)=\rho_{1,2}\left(\eta-\frac{a\xi^2}{2}\right)\exp\left(i\xi\left(b_{1,2}+a\eta-\frac{a^2\xi^2}{3}\right)\right). \tag{8}$$

Here $a$ is the free parabolic parameter, $b_{1,2}$ are the propagation constants as earlier, $\rho_{1,2}$ are the real functions. This solution assumes that pair constituents conserve an invariable profile and move along the same parabolic trajectory $\eta_p=a\xi^2/2$. The angle between the instant direction of the pair propagation and the $\xi$ axis is given by $a\xi$. Substituting (8) into the system of shortened wave equations (1) and introducing the new parabolic variable $\zeta=\eta-a\xi^2/2$, one can obtain that $\rho_{1,2}$ as the functions of new variable $\zeta$ fulfills the following system of the coupled ordinary differential equations of the second order

$$\frac{1}{2}\frac{d^2\rho_{1,2}}{d\zeta^2}=(b_{1,2}+a\zeta)\rho_{1,2}-\rho_{1,2}(\rho_1{}^2+\rho_2{}^2)+\mu\rho_{1,2}\frac{d}{d\zeta}(\rho_1{}^2+\rho_2{}^2). \tag{9}$$

This system has three nontrivial free parameters $b_{1,2}$ and $a$, but can be significantly simplified if one takes into account the fact that only the difference $\delta b=b_1$-$b_2$ between the propagation constants affects the shape of the soliton pair due to the invariance to the shift along the $\zeta$ axis. Thus the final system depends only on two parameters $\delta b,a$ and has the following form:

$$\frac{d^2\rho_1}{d\zeta^2}=2(\delta b+a\zeta)\rho_1-2\rho_1(\rho_1{}^2+\rho_2{}^2)+4\mu\rho_1\left(\rho_1\frac{d\rho_1}{d\zeta}+\rho_2\frac{d\rho_2}{d\zeta}\right),$$

$$\frac{d^2\rho_2}{d\zeta^2}=2a\zeta\rho_2-2\rho_2(\rho_1{}^2+\rho_2{}^2)+4\mu\rho_2\left(\rho_1\frac{d\rho_1}{d\zeta}+\rho_2\frac{d\rho_2}{d\zeta}\right). \tag{10}$$

Notice that the described by the Eqs. (8)–(10) theoretical approach to solution of the nonlinear Shrodinger equations in curved coordinates was first developed in [34]. In the general case of nonzero values of parameters $a$ and $\mu$ the latter system calls for the numerical integration and enables one to obtain the profiles of the stable soliton pair propagating in the PRC along the given trajectory thus supplementing the results presented above of the method of the effective par-

ticles. Further we choose as the value of the parabolic parameter the value $a=(8/15)\mu$ that describes, for example, the trajectory of the single hyperbolic-secant soliton with unity amplitude [22–25]. Performing a numerical integration we have been looking for the spatially localized pair shapes that decrease faster than arbitrary power function as $\zeta\rightarrow\pm\infty$. We used a shooting method that enables one to transform a two-point boundary problem into the Caushy problem. The initial conditions were chosen from the assumption that at $\zeta\rightarrow\pm\infty$, when amplitudes $\rho_{1,2}$ of the pair constituents are small, we can neglect nonlinear terms in Eqs. (10). Under that assumption the initial condition is given by the asymptotic of Airy function, which presents the solution of corresponding linear system

$$\frac{d^2\rho_1}{d\zeta^2}=2(\delta b+a\zeta)\rho_1,$$

$$\frac{d^2\rho_2}{d\zeta^2}=2a\zeta\rho_2, \tag{11}$$

and describes the form of nondiffracting beam in linear medium. Hence the initial values of functions and derivatives were taken in the following form:

$$\rho_1|_{\zeta=\zeta_0}=m_1\mathrm{Ai}[2(2a)^{-2/3}(\delta b+a\zeta)]|_{\zeta=\zeta_0},$$

$$\rho_2|_{\zeta=\zeta_0}=m_2\mathrm{Ai}[(2a)^{1/3}\zeta]|_{\zeta=\zeta_0},$$

$$\left.\frac{d\rho_1}{d\zeta}\right|_{\zeta=\zeta_0}=m_1\frac{d}{d\zeta}\mathrm{Ai}[2(2a)^{-2/3}(\delta b+a\zeta)]|_{\zeta=\zeta_0},$$

$$\left.\frac{d\rho_2}{d\zeta}\right|_{\zeta=\zeta_0}=m_2\frac{d}{d\zeta}\mathrm{Ai}[(2a)^{1/3}\zeta]|_{\zeta=\zeta_0}, \tag{12}$$

where $m_{1,2}$ is the new free parameters. Airy function which is widely used in quantum mechanics for description of the particle wave functions in the small regions near the turning points has a comparatively long decaying oscillating tail. However, changing the values of constants $m_{1,2}$ that determines the strength of nonlinear terms in system (10), one can compensate the oscillating tail and obtain different quasisoliton solutions.

First we considered the case of equal values of propagation constants $\delta b=b_1$-$b_2=0$ that corresponds to the one-soliton solution of the Manakov model. Further we choose the rather typical experimental value of the diffusion parameter $\mu=0.1$. The striking feature of the PRC with nonlocal component of nonlinear response is that the presence of even weak diffusion current results in the appearance of the specific multihump soliton solutions allowing different projection states just as usual Manakov solitons with shape close to the hyperbolic secant. For example such two-hump solution presented in Fig. 3 together with standard first-order soliton solution for the case of parameterization angle $\varphi=\pi/6$. The first-order soliton solution becomes slightly asymmetric due to the nonlocal component of PRC response: left wing is gently sloped than the right one. The second-order (two-hump) soliton solution consists of two partially overlapping beams. The cross-modulation coupling between them acts as an attractive force resulting in the equal self-bending despite the amplitude difference. On the left wing of the solution appears the small oscillations in accordance with asymptotic expansions (12). With the growth of $\mu$, the peaks separation increases and peaks amplitudes remain practically unchanged. It is possible to obtain more multihump solutions of the highest orders but the direct numerical simulation of the propagation of the obtained solutions shows that the higher the order of solution the more it sensitive to the perturbations due to the noise and computational errors.

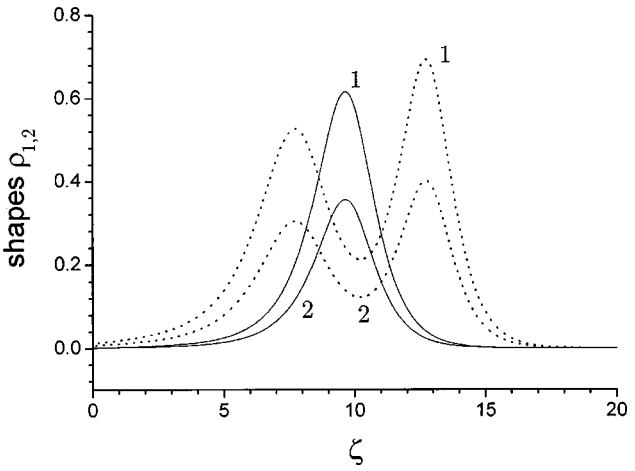


FIG. 3. First-order (straight lines) and second-order (dotted lines) soliton solutions corresponding to the zero propagation constants difference $\delta b=0$. Parameter $\mu=0.1$, parabolic parameter $a=(8/15)\mu$ and projection angle $\varphi=\pi/6$. Curves 1 depict first components $\rho_1$ and curve 2 depict second components $\rho_2$ of the solitons. All quantities are plotted in arbitrary dimensionless units.

More complicated solutions are possible for the case of nonzero propagation constants difference $\delta b$. The typical pair shapes up to the third order and corresponding refractive index profiles presented in Figs. 4–6 show rather unusual behavior with increase of propagation constant difference. For the small values of $\delta b$ the shape of the first-order solution can be approximately considered as a superposition of two slightly overlapping first-order Manakov soliton pairs with different form factors and parameterization angles (the example of the profile of such pair presented in Fig. 3 by straight lines). The form factor of the left beam is always lower than that of the right beam. With increase of $\delta b$ the overlapping between mentioned above two beams increases (compare plots (a) in Figs. 4, 5, and 6) finally resulting in practically full coincidence of the beam centers and slight asymmetry of the pair profile (plot (a) in Fig. 6). This is in good agreement with results obtained in the previous section. In accordance with Fig. 2, the higher the propagation constant difference the smaller the beam centers shift $\eta_s$ describing the profile asymmetry. Notice that despite the considerable asymmetry of the resultant shape of the first constituent, the amplitudes of two half-periods of the second constituent are practically the same. The amplitudes of first and second constituents increase with growth of $\delta b$.

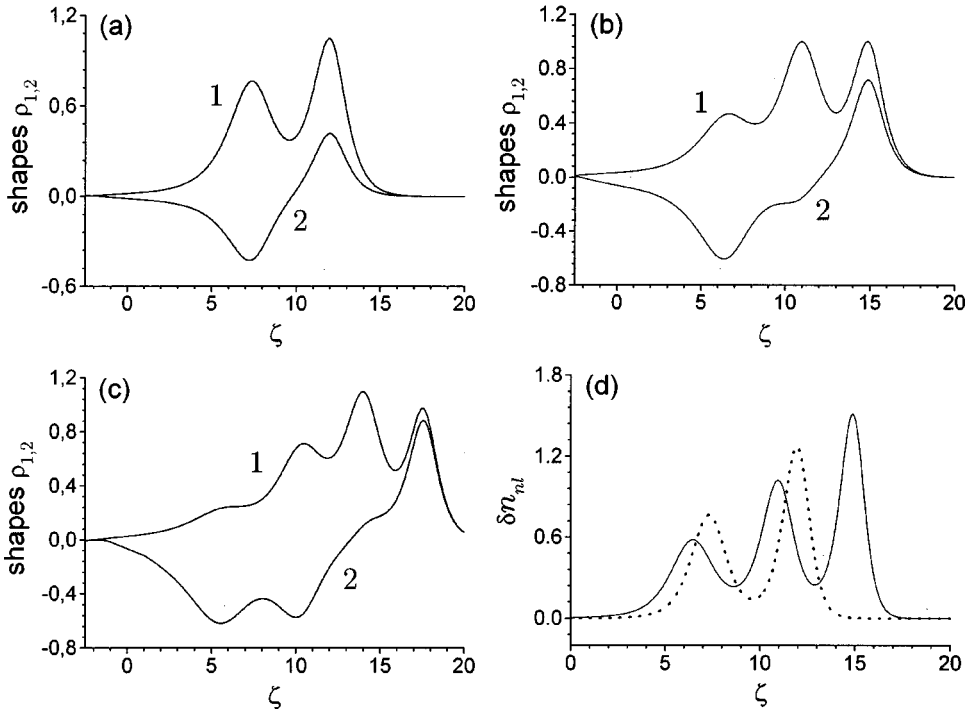


FIG. 4. First- (a), second- (b) and third-order (c) soliton solutions corresponding to the case of propagation constants difference $\delta b = 0.04$. Curves 1 depict profiles of the first soliton components $\rho_1$ and curves 2 depict profiles of the second soliton components $\rho_2$. Subfigure (d) show the refractive index profiles for the solitons of the first (dotted line) and second (straight line) orders. Diffusion parameter $\mu = 0.1$ and parabolic parameter $a = (8/15)\mu$. All quantities are plotted in arbitrary dimensionless units.

As for the case of zero value of $\delta b$ the presence of diffusion term results in the appearance of the specific multihump soliton solutions. That solutions are the analogs of the corresponding multisoliton solutions of two coupled nonlinear Shrödinger equations in the cubic medium. The nonlocal response causes of spatial separation of the components of such multisoliton complexes. The profiles of the multihump soliton pairs of the second and third orders are presented on plots (b) and (c) in Figs. 4–6. With increase of the order of solution $n$ the oscillations on the left wing become more pronounced finally resulting in transformation of the pair into the beam of infinite extent as $n$ goes to infinity. Despite the complicated profile of the higher-order pairs the corresponding refractive index profiles have very simple form presented on plots (d) in Figs. 4 and 5 for the solutions of first and second orders. One can see that the refractive index profiles for the solutions of different orders differ only by peak numbers–two for the first order, three for the second and further. The distance between neighboring peaks and refractive index modulation depth decreases with the growth

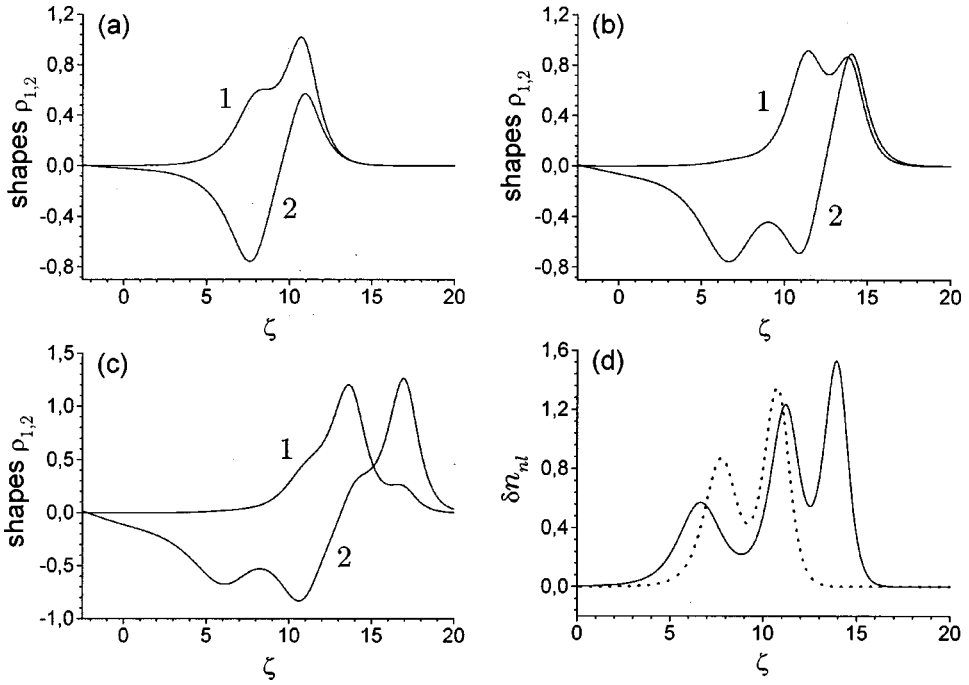


FIG. 5. First- (a), second- (b) and third-order (c) soliton solutions corresponding to the case of propagation constants difference $\delta b = 0.2$. Curves 1 depict profiles of the first soliton components $\rho_1$ and curves 2 depict profiles of the second soliton components $\rho_2$. Subfigure (d) show the refractive index profiles for the solitons of the first (dotted line) and second (straight line) orders. Diffusion parameter $\mu = 0.1$ and parabolic parameter $a = (8/15)\mu$. All quantities are plotted in arbitrary dimensionless units.

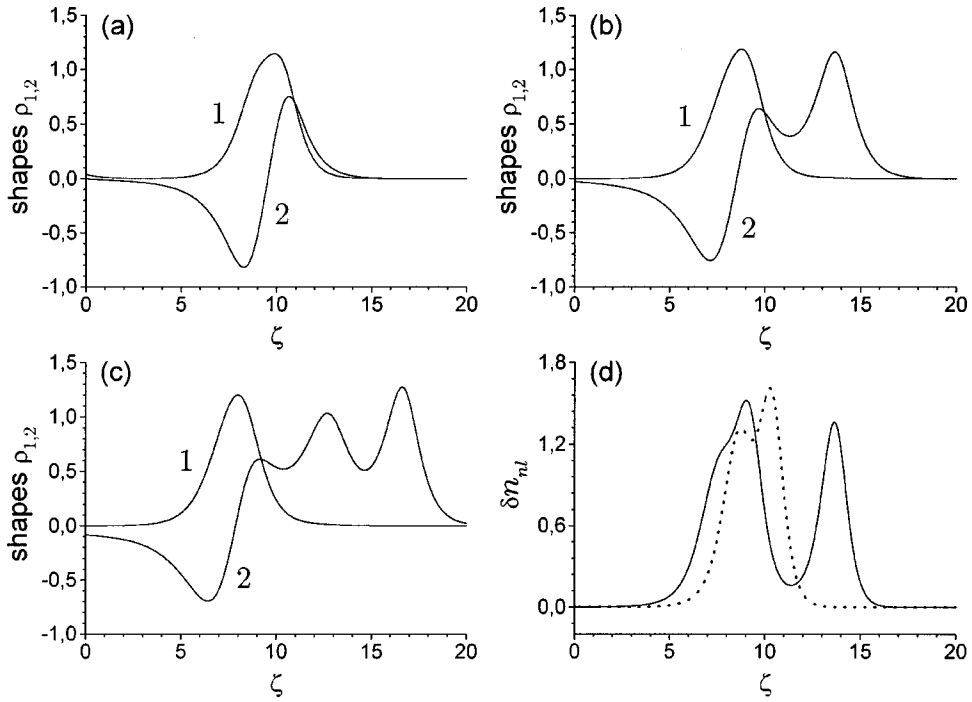


FIG. 6. First- (a), second- (b) and third-order (c) soliton solutions correspodning to the case of propagation constants difference $\delta b = 0.6$ Curve 1 depict profiles of the first soliton components $\rho_1$ and curves 2 depict profiles of the second soliton components $\rho_2$. Subfigure (d) show the refractive index profiles for the solitons of the first (dotted line) and second (straight line) orders. Diffusion parameter $\mu = 0.1$ and parabolic parameter $a = (8/15)\mu$. All quantities are plotted in arbitrary dimensionless units.

of propagation constant difference $\delta b$. Notice the rather unusual behavior of the profiles of the first and second constituents of the higher-order solutions presented in Fig. 6 that connected with the symmetrization processes occur for the big values of $\delta b$. The shape of the first constituent remains practically unchanged with the growth of the solution order $n$ and the only changes occur at the right wing of the second component which is in fact decoupled with first component due to the small value of the latter. Increase of $\delta b$ results in the further decoupling between the first and second constituents of the higher-order solutions.

With increase of the diffusion parameter $\mu$ discussed above solutions become more asymmetric. Distance between peaks of the solutions of any order increases and their amplitudes slightly decrease. When transfer into the new coordinate system corresponding to the higher value of parabolic parameter $a$ the amplitudes of the obtained solutions increase as $a^{1/4}$ and widths decrease as $a^{-1/4}$.

Further we consider the stability properties of the obtained above solutions. The stability analysis is rather complicated by both the non-Hamiltonian character of the system under consideration and the lack of analytical expression for the field spatial distribution. Therefore we consider the propagation dynamic of the soliton pairs with perturbed input profiles on the basis of the numerical simulations. The initial condition was chosen in the following way

$$q_{1,2}(\eta,0) = \rho_{1,2}(\eta) + \delta\rho(\eta), \tag{13}$$

where $\rho_{1,2}$ is the solution under consideration, $\delta\rho$ is the perturbation of the input profile. We considered both harmonic perturbation $\delta\rho = \delta\rho_0 \cos(\Omega\eta)$ and stochastic perturbation in the form of the Gaussian noise with the Lorenz correlation function $\langle \delta\rho(\eta)\delta\rho^*(\eta-\eta_0)\rangle = \sigma[1+(\eta_0/\eta_c)^2]^{-1}$, where $\sigma$ is the noise intensity and $\eta_c$ is the correlation length.

Using beam propagation method we found that the first-order soliton solutions are stable with respect to the small (up to 20% in amplitude) harmonic perturbations of the input profiles for any reasonable modulation frequencies $\Omega$ and both cases of zero and nonzero propagation constant difference $\delta b$. The typical picture of propagation dynamic of the perturbed soliton pair is depicted in Fig. 7 for the case of $\delta b = 0.2$. As one can see the soliton pair remains *structurally* stable in the process of propagation, harmonic perturbation shows the quasiperiodic behavior while its spatial scale consequently increases. One can see that the output soliton pair only changes their form factor (retaining the structure similar to input one) and thus the curvature of the trajectory over the propagation at considerable distance of 20 diffraction lengths (in experiment this corresponds to the PRC about 10 cm length) due to the additional energy contribution from the harmonic perturbation. The higher-order soliton solutions also shows good structural stability with respect to small harmonic perturbations but the numerical simulations show that the higher the order of the soliton solution the more it is sensitive to the frequency and especially the amplitude of the perturbation. Thus for example the same as for the first-order soliton perturbation can cause the slow splitting of the second-order soliton solution into the set of independent first-order Manakov pairs moving along different trajectories (see Fig. 8). Nevertheless for the small enough $\delta\rho_0$ the

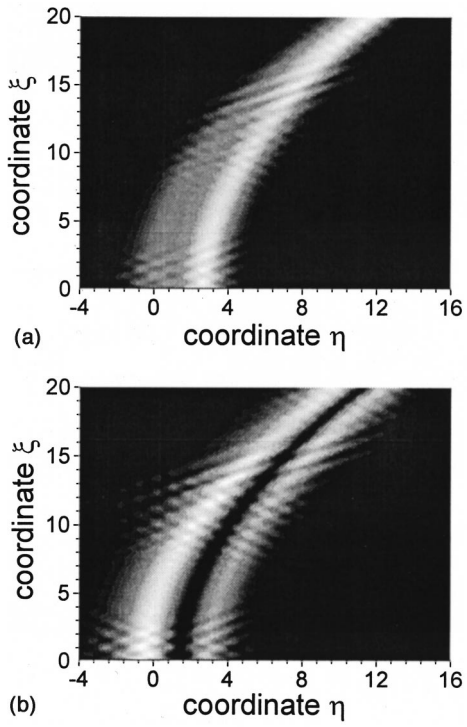


FIG. 7. Propagation dynamic of the first (a) and second (b) components of the first-order soliton pair corresponding to $\delta b = 0.2$, $\mu = 0.1$ and $a = (8/15)\mu$ in the presence of the small harmonic perturbation of the input profiles. Dimensionless modulation frequency $\Omega = 4.0$ and amplitude of perturbation $\delta\rho_0 = 0.1$. All quantities are plotted in arbitrary dimensionless units.

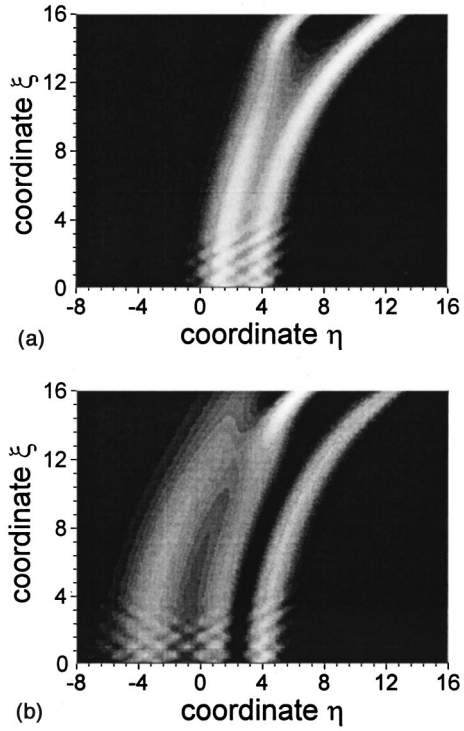


FIG. 8. Propagation dynamic of the first (a) and second (b) components of the second-order soliton pair corresponding to $\delta b = 0.2$, $\mu = 0.1$, and $a = (8/15)\mu$ in the presence of the small harmonic perturbation of the input profiles. Dimensionless modulation frequency $\Omega = 4.0$ and amplitude of perturbation $\delta\rho_0 = 0.1$. All quantities are plotted in arbitrary dimensionless units.

higher-order solitons can propagate over the significant (up to 20 diffraction lengths) distance without strong profile redistribution. We obtained analogous results concerning stability in the case of stochastic perturbation of the input profiles by a Gaussian noise.

Since we relate our discussion to the photorefractive materials (demonstrating saturation of the nonlinear response), we also consider the influence of weak saturation on the properties of the coupled soliton pairs discussed above and in addition the influence of the saturation on the structural stability of the pairs. This activity is motivated by the well-known fact [35,36] that in the case of multicomponent solitons in the local saturable medium only symmetric soliton solutions are stable. While the nonsymmetric solutions can still be found numerically, they transform into symmetric ones during propagation. If the saturation is very weak then it will take much longer distance for this transformation to occur and thus one can still talk about asymmetric solitons. We have found that in contradistinction to the case of local saturable medium the inclusion of even weak saturation in the medium with nonlocal component of the nonlinear response leads to the growth of structural stability of the self-bend soliton pairs. Numerical simulation shows the stable propagation of the perturbed asymmetric pairs in saturable medium over the distances exceeding one hundred diffraction lengths without considerable changes in shapes of the constituents. Besides, the inclusion of saturation results in considerable increase of the perturbation level necessary for destruction of the higher-order soliton pairs.

Another intriguing issue is the collision-induced pair shapes transformations in the photorefractive medium with diffusion component of nonlinear response. To study the collisions we set the initial conditions on the boundary of PRC in the following manner:

$$q_{1,2}(\eta,0) = \rho_{1,2}(\eta)\exp[-i\beta\eta + i\varphi] + \rho_{1,2}(\eta+\eta_s) \times \exp[i\beta(\eta+\eta_s)]. \quad (14)$$

Here $\rho_{1,2}$ are the profiles of the pair constituents; parameter $\eta_s$ characterizes initial spatial separation; parameter $\beta$ determines the intersection angle and $\varphi$ is the relative phase difference. The typical in-phase pair collision dynamic is shown in Fig. 9 for the first-order solution corresponding to the propagation constant difference $\delta b = 0.2$ and intersection angle $\beta = 1.0$. Because we consider here only the case of bright-bright pair interactions, the in-phase pairs attract each other as in the case of Kerr materials. The attraction is gradually being replaced by repulsion as relative phase difference increases from 0 to $\pi$. The constituents of the pairs strongly overlap even in the repulsion regime for the small intersection angles. The energy redistribution processes leading to the considerable collision induced shape transformations is much more pronounced for the pair collision in comparison with single soliton collisions. Irrespectively the solution order, relative phase difference and value of the collision angle

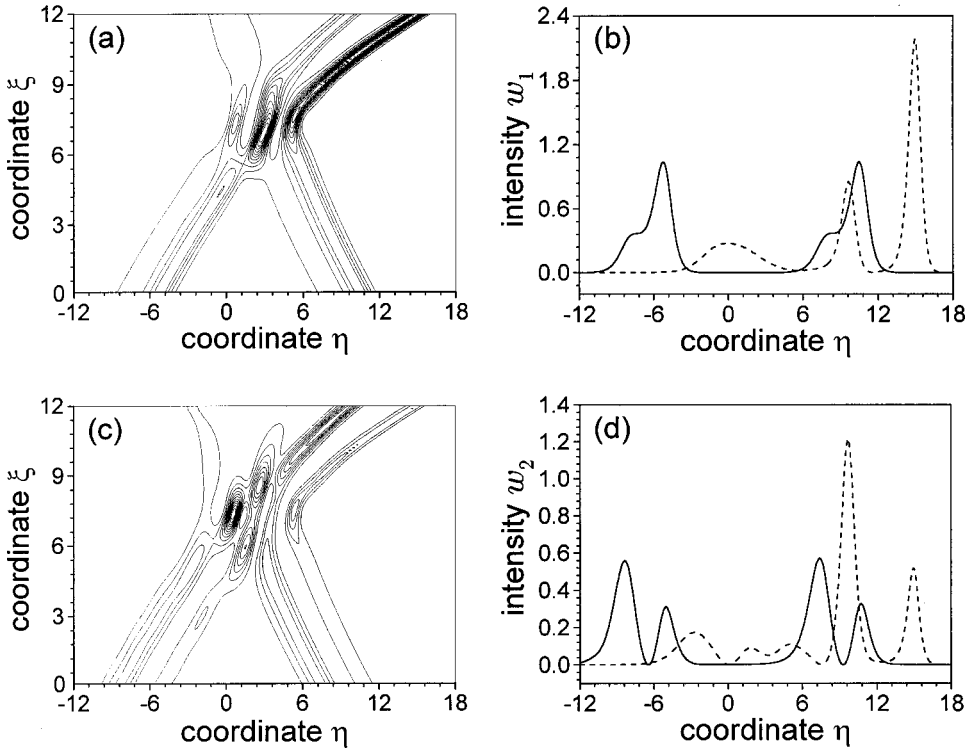


FIG. 9. In-phase collision of two first-order solitons corresponding to the case of $\delta b = 0.2$, $\mu = 0.1$, and $a = (8/15)\mu$. Intersection angle $\beta = 1.0$. Figures (a), (c) depict collision dynamic for the first and second components, respectively. Figures (b), (d) depict the input (straight lines) and output (dashed lines) intensity profiles of the first and second components, respectively. All quantities are plotted in arbitrary dimensionless units.

the pair collision causes of splitting into the two (or more) Manakov soliton pairs of the first order (see Figs. 9(b) and 9(d) that show the output intensity profiles of the first and second components). Together with the results concerning stability of the obtained above solutions this means that Manakov soliton pair is the most stable structure in the medium with nonlocal component of nonlinear response. The resultant number of the Manakov pairs strongly depends from the order of the colliding soliton pairs and intersection angles but practically independent on relative phase difference. The last one strongly affects only the amplitudes of the pairs born upon collision and dynamic in the area of the intersection. Thus the collision of two identical first-order Manakov pairs causes of appearance of two pairs with different energies if intersection angle $\beta < 3.0$. For the higher values of $\beta$ it is possible birth of up to four pairs. Collision of the solitons corresponding to the nonzero $\delta b$ always results in the appearance of more than two Manakov pairs. For the small angles (for example for the collision of the two first-order pairs corresponding to $\delta b = 0.2$ angle $\beta$ should be less than approximately 2.0) usually appear three Manakov pairs (see Fig. 9). As angle and colliding solitons order (in fact the increase of the order means the increase of the overall energy used in collision) increases the number of pairs that can be born upon collision increase and can reach five or more. The variety of the energy redistribution processes occur under the pair collision in the PRC with diffusion current make such medium especially attractive for the optical devices construction.

## V. CONCLUSION

To summarize the paper, let us briefly list our main results and conclusions. By the effective particle method, we have shown that in the presence of the drift component of nonlinearity the Manakov's pair propagates along the parabolic trajectory with the coefficient given by Eq. (5) and remains stable. In the case of asymmetric initial conditions [Eq. (4)] it was found that for definite values of propagation constant the quasistable propagation of both constituents of the soliton pair along the parabolic trajectory is also possible. The system of equations describing the profiles of the coupled soliton pairs was solved numerically in curved coordinates. The single soliton solution is slightly asymmetric and the multisoliton solution looks like a multihumped beam. The stability analysis has shown that this single-soliton solution shows structural stability with respect to the small perturbations but the multisoliton solution is more sensitive to the perturbations and shows tendency to the splitting into the set of Manakov's pairs. During the collision, the energy redistribution processes lead to the considerable transformation of the profiles of the resulting beams with the obvious tendency to the several stable Manakov pairs formation.

[1] B. Crosignani, M. Segev, D. Engin, P. Di Porto, A. Yariv, and G. Salamo, J. Opt. Soc. Am. B **10**, 446 (1993).

[2] G. Duree, M. Morin, G. Salamo, M. Segev, B. Crosignani, P. Di Porto, E. Sharp, and A. Yariv, Phys. Rev. Lett. **74**, 1978 (1995).

[3] M. Iturbe-Castillo, P. Marques-Aquilar, J. Sanchez-Mondragon, S. Stepanov, and V. Vysloukh, Appl. Phys. Lett. **64**, 408 (1994).

[4] V. Kutuzov, V. Petnikova, V. Shuvalov, and V. Vysloukh, Phys. Rev. E **57**, 6056 (1998).
[5] D. Christodoulides and M. Carvalho, J. Opt. Soc. Am. B **12**, 1628 (1995).
[6] Z. Chen, M. Segev, T. Coskun, D. Christodoulides, Y. Kivshar, and V. Afanasjev, Opt. Lett. **21**, 1821 (1996).
[7] Z. Chen, M. Segev, S. Singh, T. Coskun, and D. Christodoulides, J. Opt. Soc. Am. B **14**, 1407 (1997).
[8] A. Zozulya, D. Anderson, A. Mamaev, and M. Saffman, Phys. Rev. A **57**, 522 (1998).
[9] S. Bian, J. Frejlich, and K. Ringhofer, Phys. Rev. Lett. **78**, 4035 (1997).
[10] G. Garcia-Quirino, M. Iturbe-Castillo, V. Vysloukh, and S. Stepanov, Opt. Lett. **22**, 154 (1997).
[11] W. Krolikowski, B. Luther-Davies, C. Denz, and T. Tschudi, Opt. Lett. **23**, 97 (1998).
[12] W. Krolikowski and S. Holmstrom, Opt. Lett. **22**, 369 (1997).
[13] A. Mamaev, M. Saffman, and A. Zozulya, J. Opt. Soc. Am. B **15**, 2079 (1998).
[14] E. Ostrovskaya and Y. Kivshar, Opt. Lett. **23**, 1268 (1998).
[15] W. Krolikowski, M. Saffman, B. Luther-Davies, and C. Denz, Phys. Rev. Lett. **80**, 3240 (1998).
[16] V. Kutuzov, V. Petnikova, V. Shuvalov, and V. Vysloukh, J. Nonlinear Opt. Phys. Mater. **6**, 421 (1997).
[17] D. Christodoulides and T. Coskun, Opt. Lett. **19**, 1714 (1994).
[18] Z. Sheng, Y. Cui, N. Cheng, and Y. Wei, J. Opt. Soc. Am. B **13**, 584 (1996).
[19] D. Christodoulides and T. Coskun, Opt. Lett. **21**, 1220 (1996).
[20] D. Christodoulides and T. Coskun, Opt. Lett. **21**, 1460 (1996).
[21] J. Hermann and S. Gatz, Opt. Lett. **23**, 1176 (1998).
[22] W. Krolikowski, N. Akhmediev, B. Luther-Davies, and M. Cronin-Golomb, Phys. Rev. E **54**, 5761 (1996).
[23] N. Akhmediev, W. Krolikowski, and A. Lowery, Opt. Commun. **131**, 260 (1996).
[24] Y. Kodama and K. Nozaki, Opt. Lett. **12**, 1038 (1987).
[25] Y. Kodama and A. Hasegawa, IEEE J. Quantum Electron. **23**, 510 (1987).
[26] S. Manakov, Sov. Phys. JETP **38**, 248 (1974) [Zh. Eksp. Teor. Fiz. **65**, 505 (1974)].
[27] J. Kang, G. Stegeman, J. Aitchison, and N. Akhmediev, Phys. Rev. Lett. **76**, 3699 (1996).
[28] M. Morin, G. Duree, G. Salamo, and M. Segev, Opt. Lett. **20**, 2066 (1995).
[29] N. Akhmediev, V. Eleonskii, N. Kulagin, and L. Shil'nikov, Sov. Tech. Phys. Lett. **15**, 587 (1989).
[30] N. Akhmediev and A. Ankiewicz, *Solitons, Nonlinear Pulses and Beams* (Chapman & Hall, London, 1997).
[31] N. Akhmediev, W. Krolikowski, and A. Snyder, Phys. Rev. Lett. **81**, 4632 (1998).
[32] M. Iturbe-Castillo, M. Torres-Cisneros, J. Sanchez-Mondragon, S. Chavez-Cerda, S. Stepanov, V. Vysloukh, and G. Torres-Cisneros, Opt. Lett. **20**, 1853 (1995).
[33] A. Snyder and Y. Kivshar, J. Opt. Soc. Am. B **14**, 3025 (1997).
[34] L. Gagnon and P. Belanger, Opt. Lett. **15**, 466 (1990).
[35] W. Krolikowski, N. Akhmediev, and B. Luther-Davies, Phys. Rev. E **59**, 4654 (1999).
[36] N. Litchinitser, W. Krolikowski, N. Akhmediev, and G. Agrawal, Phys. Rev. E **60**, 2377 (1999).